Journal of Coordination Chemistry

ISSN: 0095-8972 (Print) 1029-0389 (Online) Journal homepage: http://www.tandfonline.com/loi/gcoo20

Kinetics of the reaction of nitric oxide with polypyridylamine iron(II) complexes

Federico Roncaroli & Roland Meier

To cite this article: Federico Roncaroli & Roland Meier (2015) Kinetics of the reaction of nitric oxide with polypyridylamine iron(II) complexes, Journal of Coordination Chemistry, 68:17-18, 2990-3002, DOI: 10.1080/00958972.2015.1057710

To link to this article: http://dx.doi.org/10.1080/00958972.2015.1057710

Accepted author version posted online: 03 Jun 2015.
Published online: 30 Jun 2015.

Journal of Coordination Chemistry, 2015
Vol. 68, Nos. 17–18, 2990–3002, http://dx.doi.org/10.1080/00958972.2015.1057710

Kinetics of the reaction of nitric oxide with polypyridylamine iron(II) complexes

FEDERICO RONCAROLI*† and ROLAND MEIER‡

†Departamento de Física de la Materia Condensada, Centro Atómico Constituyentes, Comisión Nacional de Energía Atómica, Buenos Aires, Argentina
‡Zentrum für Angewandte Forschung, Technische Hochschule Ingolstadt, Ingolstadt, Germany

(*Received 20 February 2015; accepted 23 April 2015*)

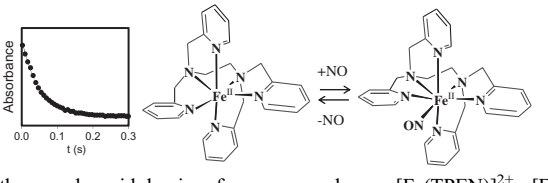

The reactions of three polypyridylamine ferrous complexes, $[Fe(TPEN)]^{2+}$, $[Fe(TPPN)]^{2+}$, and $[Fe(TPTN)]^{2+}$, with nitric oxide (NO) (where TPEN = *N,N,N′,N′*-tetrakis(2-pyridylmethyl)ethylenediamine, TPPN = *N,N,N′,N′*-tetrakis(2-pyridylmethyl)-1,2-propylenediamine, and TPTN = *N,N,N′,N′*-tetrakis(2-pyridylmethyl)trimethylenediamine) were investigated. The first two complexes, which are spin-crossover systems, presented second-order rate constants for complex formation reactions (k_f) of 8.4×10^3 and 9.3×10^3 M^{-1} s^{-1}, respectively (pH 5.0, 25 °C, $I = 0.1$ M). In contrast, the $[Fe(TPTN)]^{2+}$ complex, which is in low-spin ground state, did not show any detectable reaction with NO. k_f values are lower than those of high-spin Fe(II) complexes, such as $[Fe(EDTA)]^{2-}$ (EDTA = ethylenediaminetetraacetate) and $[Fe(H_2O)]^{2+}$, but higher than low-spin Fe(II) complexes, such as $[Fe(CN)_5(H_2O)]^{3-}$ and $[Fe(bipyridine)_3]^{2+}$. The release of NO from the $[Fe(TPEN)NO]^{2+}$ and $[Fe(TPPN)NO]^{2+}$ complexes were also studied, showing the values 15.6 and 17.7 s^{-1}, respectively, comparable to the high-spin aminocarboxylate analogs. A mechanism is proposed based on the spin-crossover behavior and the geometry of these complexes and is discussed in the context of previous publications.

Keywords: Nitrosyl; Spin-crossover; NO; Non-heme; Fe

1. Introduction

In the 1980s, it was discovered that nitric oxide or nitrogen monoxide (NO) is generated in mammalian cells playing important roles in many biological processes. Most of these functions involve the reaction of NO with metal centers present in proteins [1, 2].

From a different approach, NO is a pollutant generated in industrial processes, particularly during combustion of nitrogenated organic substances [3]. This led to significant research concerning the design of possible scavengers that can react with NO

*Corresponding author. Email: roncaroli@cnea.gov.ar

and eventually convert it to less toxic species such as N_2 or N_2O [4–6]. For example, the iron(II) complex with ethylenediaminetetraacetate (EDTA) has been proposed as a NO-scavenger [7].

Much research has been done on the reactivity between NO and related aminocarboxylate (non-heme) iron complexes [4–7]. Some ligands have been synthesized, where carboxylate groups in polyaminocarboxylate have been substituted by pyridyl groups, which are the subject of this report. Nitrosyl metal complexes with ligands such as TPEN (*N,N,N′,N′*-tetrakis(2-pyridylmethyl)ethylenediamine), PIDA (2-pyridylmethyl-iminodiacetate), and EDAMPDA (*N,N′*-bis(pyridylmethyl)ethylenediamine-*N,N′*-diacetate) were prepared and characterized by spectroscopic techniques [8, 9]. Some of them exhibit the unusual $S = 3/2$ ground state, while others have $S = 1/2$ spin state [8, 9]. Ligand field factors promoting one ground state over the other have been investigated [10–15]. Although some studies deal with the reaction of NO with this sort of complexes [8–10], as far as we know, no kinetic studies were done.

The $[Fe^{II}(TPEN)]^{2+}$ complex, in solution, was the first rapidly interconverting (18 ns) ferrous spin-crossover compound studied [16, 17], with a $^1A_1$ ground state and a thermally accessible $^5T_2$ excited state. The increase in Fe–N bond lengths together with an increase in the trigonal distortion led to the fast rate of spin-state interconversion in $[Fe^{II}(TPEN)]^{2+}$ [18–21]. The steric constraints introduced by the hexadentate ligand led to a relatively large trigonal distortion lowering the energy of triplet excited states ($^3T_1$ and/or $^3T_2$). This leads to greater spin-orbit interaction of the $^1A_1$ low-spin state with components of the $^5T_2$ high-spin state, resulting in a greater rate of interconversion between high- and low-spin states [18–21]. The interpretation of the experimental data has been supported by DFT calculations [22–24]. Interestingly, the Fe(II) tetrakis-*N,N,N′,N′*-(2-pyridylmethyl)trimethylenediamine complex, $[Fe^{II}TPTN]^{2+}$, which has a much smaller trigonal distortion, is in the low-spin state at least up to 400 K [19, 21]. In solution, $[Fe^{II}(TPEN)]^{2+}$ exhibits a very fast rate (>600 s^{-1}) of enantiomerization. It has been suggested that spin equilibrium is coupled with this enantiomerization mechanism [18, 21].

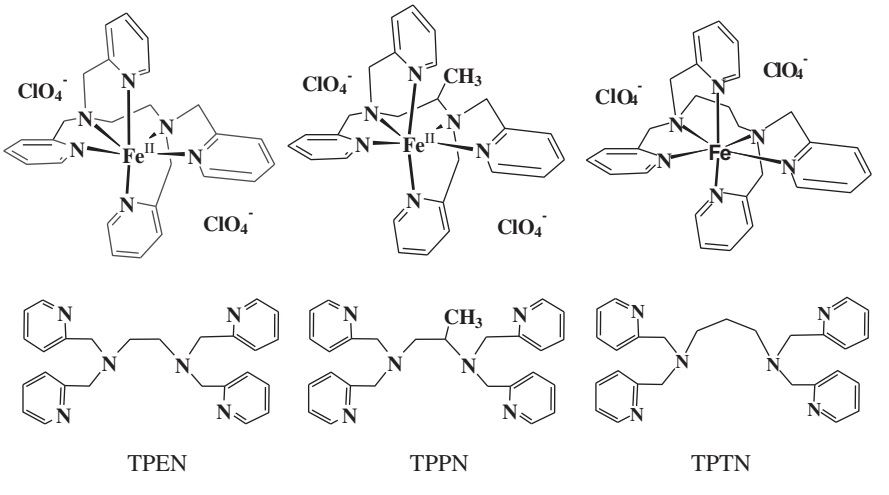

Figure 1. Ligands and complexes employed in this study.

It was also found that these complexes display superoxide dismutase (SOD) activity and can activate O_2 and H_2O_2 [25–30]. The $[Fe^{II}TPTN]^{2+}$ complex does not show SOD activity, probably because this last complex has undistorted steric structure with no easily substituted ligand [27]. In contrast, $[Fe^{II}(TPEN)]^{2+}$, which displays a higher distortion facilitating ligand substitution, displays a high SOD activity [27–29]. Nitrosyl complexes have been proposed as stable analogs of possible oxygen intermediates in the non-heme iron enzymes [11, 12].

In this report, a kinetic study was performed on the reaction of NO with Fe(II) complexes of the following ligands: TPEN, TPPN (*N,N,N′,N′*-Tetrakis(2-pyridylmethyl)-1,2-propylenediamine), and TPTN, which are shown in figure 1. The kinetic data were interpreted and discussed in terms of the electronic and crystal structure of these complexes, the spin equilibrium, and previous kinetic results on aminocarboxylate complexes. Finally, a possible mechanism was proposed.

2. Experimental

2.1. *Materials*

NO 99.9% was purchased from Alpha Caz and purified from higher nitrogen oxides by passing through an Ascarite II (Aldrich) column.

TPEN (*N,N,N′,N′*-tetrakis(2-pyridylmethyl)-1,2-ethylenediamine), TPPN (*N,N,N′,N′*-tetrakis(2-pyridylmethyl)-1,2-propylenediamine), TPTN (*N,N,N′,N′*-tetrakis(2-pyridylmethyl)-1,3-propylenediamine), $[Fe(TPEN)](ClO_4)_2$, $[Fe(TPPN)](ClO_4)_2$, and $[Fe(TPTN)](ClO_4)_2$ were prepared as described in the literature, and purity was checked by elemental analysis [16].

$NaNO_2$ was purchased from Merck. The rest of the chemicals were of analytical grade and used without purification.

2.2. *Methods*

All the solutions were prepared using distilled and purified water (Milli-Q system) deoxygenated with N_2-saturation in Schlenk tubes and handled with gastight syringes. Citrate (pH 3), acetate (pH 5), bis-tris (bis[2-hydroxyethyl]imino-tris[hydroxymethyl]methane) (pH 7), and borate (pH 10) were always used to control the pH. $HClO_4$ solutions were also used at pH 3. The ionic strength was adjusted with $NaClO_4$. NO-saturated solutions were prepared by slow bubbling of NO through deoxygenated buffer or complex solutions. The NO concentration of such solutions is already known from our previous work, viz. 1.8 mM at 25 °C [6, 7, 31]. These solutions were eventually diluted with buffer solutions to reach the final desired NO concentration.

Complex solutions were prepared by dissolving $[Fe(TPEN)](ClO_4)_2$, $[Fe(TPPN)](ClO_4)_2$, or $[Fe(TPTN)](ClO_4)_2$ in the corresponding buffer or $HClO_4$ solutions or, alternatively, by dissolving the required amount of $Fe(BF_4)_2{\cdot}6H_2O$ and two- to five-fold excess of TPEN, TPPN, or TPTN in the buffer or acid solution. No significant differences were observed using both methods.

The UV–vis spectral changes during the reaction between NO and the studied complexes were recorded on a Varian Cary 5G spectrophotometer. The complex solutions (20 mL, 1×10^{-4} M) were placed in a 1-cm quartz cuvette directly attached to a 50-mL round flask with sideway gas connections. NO was bubbled through the solutions during 5 min, and then, N_2 was bubbled for 3 min. The UV–vis spectra were recorded after each procedure, and the complete cycle could be repeated several times.

The pH measurements were done with a WTW InoLab level 1 pH meter at room temperature.

The electron paramagnetic resonance (EPR) spectrum of a frozen $Fe(TPEN)^{2+}$ solution saturated with NO (1.1×10^{-3} M in Fe, 3.3×10^{-3} M in TPEN, pH 5.0, 0.1 M in acetate buffer) was measured on the X-band of a Bruker ESP 300E spectrometer at T 132 K. The spectrum was recorded at 9.41 GHz, 6.35 mW power, 100 kHz modulation frequency, and 9.434 G modulation amplitude. Simulations were performed by the EasySpin program [32] written in MATLAB (Mathworks). The expression of the spin Hamiltonian (H_e) employed to simulate this spectrum is described in Equation (1) [33].

$$H_e = D\left[S_z^2 - S(S+1)/3 + (E/D)\left(S_x^2 - S_y^2\right)\right] + \mu_B \boldsymbol{B}\boldsymbol{g}\boldsymbol{S} \quad (1)$$

In equation (1), $\boldsymbol{B}$ is the external magnetic field. $\boldsymbol{S}$ is the electronic spin operator (vector), and S_x, S_y, and S_z are its components. S equals 1/2 (low spin) or 3/2 (high spin) in this report. D and E/D are the axial and rhombic zero-field splitting parameters, respectively, for $S > 1/2$. μ_B is the Bohr magneton, and $\boldsymbol{g}$ is the matrix that describes the electron Zeeman interaction.

2.3. *Kinetic experiments*

Stopped-flow measurements were carried out on a SX-18 MV stopped-flow spectrophotometer from Applied Photophysics at 25.0 ± 0.1 °C. Kinetic traces were monitored at 414, 417, and 425 nm for $[Fe(TPEN)]^{2+}$, $[Fe(TPPN)]^{2+}$, and $[Fe(TPTN)]^{2+}$, respectively. They were fitted to a single exponential function at least 3 half-lives, usually 5, with the SX-18 MV program. The reported observed rate constants (k_{obs}) are the averages of 6–12 kinetic runs, and the errors correspond to the standard deviation of the data.

Some preliminary experiments were carried out for the reaction of NO with $[Fe(TPEN)]^{2+}$ at pH 3.0, 5.0, 7.0, and 10.0. The final Fe concentration was $5–6 \times 10^{-5}$ M, the final NO concentration was 9.0×10^{-4} M, and the buffer concentration was 0.1 M. The influence of the presence of free NO_2^- in the NO solution was studied (final $[NO_2^-]$ 4.9×10^{-3} M, pH 7.0, 0.1 M bis-tris). A complementary experiment at 1.0 M ($NaClO_4$) ionic strength was also done (pH 7.0, 0.1 M bis-tris). For the same complex, the NO-concentration dependence of the formation rate constant was studied at pH 3.0, 5.0, and 7.0; the ionic strength was 0.1 M ($NaClO_4$); and the buffer concentration was 0.01 M (at pH 3.0, $HClO_4$ was used instead of citrate buffer). The final Fe concentration was $2–6 \times 10^{-5}$ M, and the final NO concentration was $2.3–9.0 \times 10^{-4}$ M. The NO-concentration dependence of the formation rate constant for $[Fe(TPPN)]^{2+}$ was studied at pH 5.0 in the same way as described before. Finally, attempts to study the reactivity of $[Fe(TPTN)]^{2+}$ against NO were done at pH 5.0 (I 0.1 M, 0.01 M acetate buffer, 9.0×10^{-4} M NO).

The complex dissociation reaction was studied for $[Fe(TPEN)]^{2+}$. For this purpose, the $[Fe(EDTA)]^{2-}$ complex (EDTA = ethylenediaminetetraacetate) was used as NO-scavenger as described in the literature [6, 7, 31, 34]. The solutions of this last compound were prepared in the following way: 50 and 70 mg of $FeSO_4 \cdot 7H_2O$ and 100 and 140 mg of ethylenediaminetetraacetic acid, respectively, were dissolved in 20 mL of 0.1 M bis-tris buffer solution (pH 7.0). After this procedure, the pH was readjusted. A solution 1.0×10^{-4} M in $[Fe(TPEN)]^{2+}$ was saturated with NO (pH 7.0, 0.01 M bis-tris buffer, I 0.1 M). Finally, equal volumes of the two solutions were mixed in the stopped-flow apparatus. Some complementary experiments were done using $[Fe(H_2O)_6]^{2+}$ as NO-scavenger. A solution 2.6×10^{-4} M in $[Fe(TPEN)]^{2+}$ was saturated with NO (pH 5.0, 0.01 M acetate buffer, I 0.1 M). A 1 : 4 dilution of this last solution was mixed in the stopped-flow apparatus with an equal volume of a solution of $FeSO_4 \cdot 7H_2O$ (2.5, 4.6, and 7.3×10^{-3} M) in the same buffer.

3. Results: NO reactivity, formation, and dissociation reactions

Figure 2 shows the UV–vis spectral changes corresponding to the reaction between $[Fe(TPEN)]^{2+}$ and NO. The band at 414 nm ($\varepsilon = 1.0 \times 10^4$ M^{-1} cm^{-1}, in agreement with literature data) [16] decreases to one half upon NO bubbling. The depletion of this band can be interpreted in terms of the conversion into the nitrosylated complex. A ratio close to 1 : 1 between the reactant and the nitrosylated compound is expected for an NO-saturated solution (1.8×10^{-3} M), since an equilibrium constant K_{eq} (see equation (1)) of 560 M^{-1} can be estimated from the kinetic data (i.e., k_f/k_d, *vide infra*). Through N_2-bubbling, the spectral changes can be reversed, and the reaction is reversible. A slight increase in the band intensity at the end of the experiment can be ascribed to solvent evaporation during

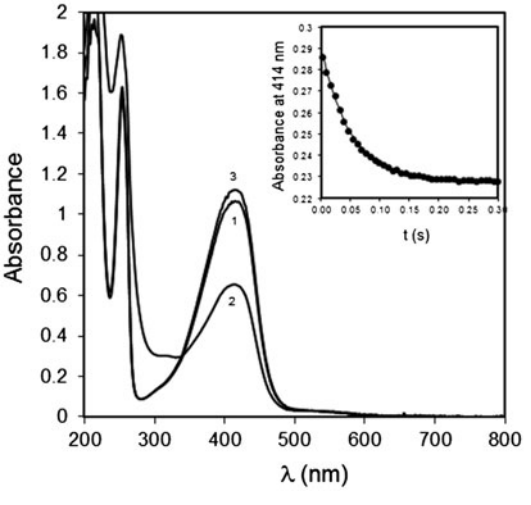

Figure 2. UV–vis spectral changes corresponding to reaction of $[Fe(TPEN)]^{2+}$ with NO. (1) Spectrum of a solution 1.0×10^{-4} M in $[Fe(TPEN)]^{2+}$ (pH 5.0, 0.1 M acetate buffer, $T = 25$ °C), (2) spectrum of the last solution saturated with NO (5 min), and (3) spectrum of the last solution after N_2 saturation (3 min). Inset: kinetic trace at 414 nm during the reaction with NO, $k_{obs} = 20.4$ s^{-1}, ([NO] = 6.8×10^{-4} M, [complex] = 3.0×10^{-5} M, pH 5.0, [acetate buffer] = 0.01 M, $I = 0.1$ M, $T = 25.0$ °C).

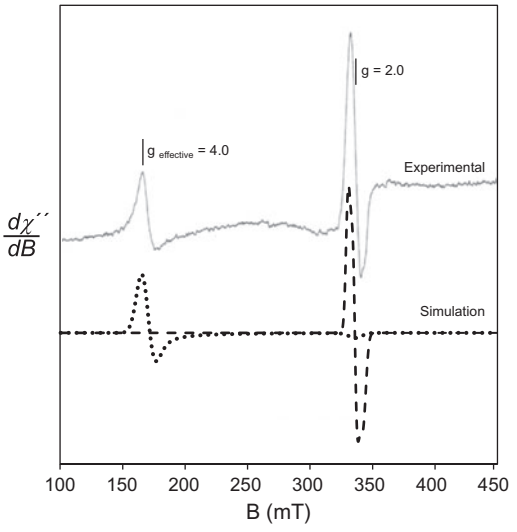

Figure 3. X-band EPR spectrum of a $[Fe(TPEN)]^{2+}$ complex solution saturated with NO (1.1×10^{-3} M in Fe, 3.3×10^{-3} M in TPEN, pH 5.0, 0.1 M in acetate buffer, measured at T 132 K). Solid line: experimental spectrum: 9.41 GHz, 6.35 mW power, 100 kHz modulation frequency, and 9.434 G modulation amplitude. Dotted line: simulated spectrum with parameters: $S = 3/2$, $g = 2.0$, $D = 12.6$ cm^{-1}, $E = 0$ cm^{-1}, line width = 12 mT. Dashed line: simulated spectrum with parameters: $S = 0.5$, $g = (2.035, 2.001, 1.962)$, line width = 4 mT, g-strain = (0, 0, 0.022).

NO/N_2 bubbling. This procedure was repeated several times, supporting the reversibility of the reaction. Similar spectral changes were observed for the $Fe(TPPN)]^{2+}$ complex (not shown). In contrast, no appreciable changes were detected with $Fe(TPTN)]^{2+}$.

The X-band EPR spectrum of a $[Fe(TPEN)]^{2+}$ complex solution saturated with NO measured at 132 K is shown in figure 3. Two signals were detected. The spin Hamiltonian parameters employed to simulate the high field part of the spectrum were $S = 1/2$ and $g = (2.035, 2.001,$ and $1.962)$, which correspond to a low-spin system and are in agreement with the previous report for $[Fe(TPEN)NO]^{2+}$ [8]. At lower fields, another signal was observed, which was simulated with the parameters $S = 3/2$, $g = 2.0$, $D = 12.6$ cm^{-1}, and $E = 0$ cm^{-1}. These parameters correspond to an effective g *ca.* 4.0 as previously found with some nitrosyl–aminocarboxylate complexes, including $[Fe(EDTA)NO]^{2-}$, and does not correspond to adventitious high-spin Fe^{III} ($S = 5/2$) species which exhibit g effective values 5–8 [8, 13]. However, this low field signal has not been previously observed for the $[Fe(TPEN)NO]^{2+}$ complex at 105 K [8]. If this last complex is a spin-crossover system as the parent compound, it is reasonable that a high-spin ($S = 3/2$) ground state can be reached at higher temperature.

In this way, the reaction with NO can be considered as equilibrium and is formulated as in equation (2).

$$[Fe(L)]^n + NO \underset{k_d}{\overset{k_f}{\rightleftharpoons}} [Fe(L)(NO)]^n \quad K_{eq} \tag{2}$$

Equation (2) represents our reaction of interest. L corresponds to TPEN and TPPN (see Experimental section), k_f is the nitrosyl complex formation rate constant, and k_d is the complex dissociation rate constant, i.e., the dissociation of NO. K_{eq} can be estimated as

k_f/k_d. Under pseudo-first-order conditions, i.e., excess of NO (the concentration remains approximately constant during the NO binding reaction), the observed rate constant for the depletion of the $[Fe(TPPN)]^{2+}$ complex, k_{obs}, should depend linearly on the NO concentration according to equation (3), with a slope equal to k_f and an intercept equal to k_d.

$$k_{obs} = k_f[NO] + k_d \quad (3)$$

The inset in figure 2 shows the stopped-flow kinetic trace during the reaction of NO with $[Fe(TPEN)]^{2+}$. All the kinetic traces showed first-order behavior under excess of NO; in this way, the observed rate constant values (k_{obs}) were determined. We carefully checked the influence of several factors on k_{obs}. These values are independent of the pH (5–10), the buffer concentration (0.1–0.01 M), and the ionic strength (1.0–0.1 M). The presence of NO_2^- (4.9×10^{-3} M) did not show appreciable effect on k_{obs}. This last finding is relevant since NO_2^- is usually present in NO solutions and it was asserted that it can catalyze the reaction with NO under certain conditions [35].

Figure 4 shows the NO-concentration dependence of k_{obs} for $[Fe(TPEN)]^{2+}$ and $[Fe(TPPN)]^{2+}$. Stopped-flow experiments showed that $[Fe(TPTN)]^{2+}$ does not react with NO, which is in agreement with the experiments done with the spectrophotometer. All the data displayed linear distributions with appreciable intercepts that can be analyzed in terms of equation (3). The data for $[Fe(TPEN)]^{2+}$ showed very similar slopes and intercepts at pH 7.0 and 5.0, viz. 8900 ± 400 M^{-1} s^{-1} and 15.0 ± 0.3 s^{-1}, and 8400 ± 900 M^{-1} s^{-1} and 15.6 ± 0.6 s^{-1}, respectively. No acid catalysis could be detected in the reactivity toward NO; moreover, there is no evidence of protonation of pyridyl groups during the reaction. The $[Fe(TPPN)]^{2+}$ complex was studied only at pH 5.0, and it showed very similar values to the ones found for $[Fe(TPEN)]^{2+}$, viz. 9300 ± 900 M^{-1} s^{-1} and 17.7 ± 0.5 s^{-1}, slope and intercept, respectively.

Finally, the complex dissociation reaction (k_d) was directly measured for $[Fe(TPEN)]^{2+}$, using a NO-trap or NO-scavenger, as reported [6, 7, 31, 34]. Under sufficiently large scavenger concentrations, the reaction is controlled by the complex dissociation reaction

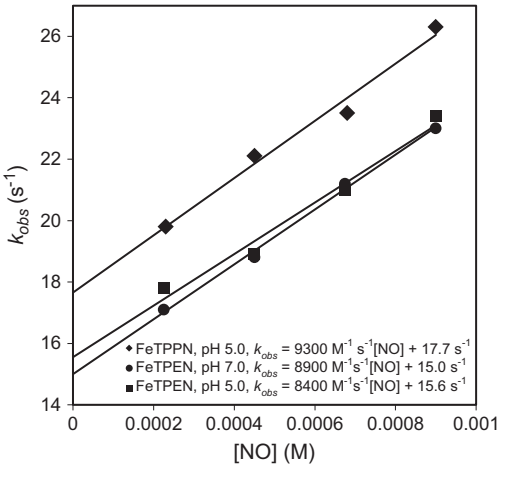

Figure 4. NO-concentration dependence of the observed rate constant (k_{obs}) for reaction of the $[Fe(TPEN)]^{2+}$ and $Fe(TPPN)]^{2+}$ complexes with NO. ([complex] = 2–6 × 10^{-5} M, [NO] = 2.3–9.0˟10^{-4} M, [buffer] = 0.01 M, I = 0.1 M, T = 25.0 °C).

($k_{obs} = k_d$). In our study, $[Fe(EDTA)]^{2-}$ was employed as NO-scavenger. For $[Fe(EDTA)]^{2-}$ concentrations of 9.0×10^{-3} M and 12.5×10^{-3} M, k_{obs} was 18 ± 1 and 16 ± 2 s^{-1}, respectively. These data, in agreement with the intercepts observed in figure 4, give strong support to the model described in equation (1). In order to discard the possible reaction between excess EDTA and $[Fe(TPEN)NO]^{2+}$, $[Fe(H_2O)_6]^{2+}$ was used as scavenger. For concentrations of 2.5, 4.6, and 7.3×10^{-3} M, the observed rate constants were 18.2 ± 0.4, 17.1 ± 0.9, and 17.0 ± 0.8 s^{-1}, respectively, which is in reasonable agreement with the previously discussed data.

4. Discussion: the mechanism

Table 1 shows the kinetic data for the NO complex formation reaction with the $[Fe(TPEN)]^{2+}$ and $[Fe(TPPN)]^{2+}$ complexes together with literature data, particulary Fe(II) high-spin aminocarboxylate complexes. It is possible to observe that $[Fe(TPEN)]^{2+}$ and $[Fe(TPPN)]^{2+}$ fall between the typical high-spin complexes (aminocarboxylate ligands) and the low-spin $[Fe^{II}(CN)_5(H_2O)]^{3-}$ and $[Fe(bipy)_3]^{2+}$ complexes. The Fe porphyrin complex, $Fe^{II}(TPPS)$, is a special case since it is five-coordinate and the reaction with NO is diffusion-controlled [37]. [The $Fe^{II}(bipy)_3]^{2+}$ (bipy = 2,2′-bipyridine) complex displays a $S = 0$ ground state [36, 38]. The very slow reactions with cyanide and other incoming ligands were studied for this last compound, proving to be independent of the entering ligand, and being controlled by the dissociation of one of the pyridyl groups through a dissociative mechanism [38]. Since it is independent of the incoming ligand, a comparison with the NO reactions is reasonable. The $[Fe^{II}(CN)_5(H_2O)]^{3-}$ complex is the other rare low-spin Fe(II) system whose reaction with NO was studied [31]. In this case, the reaction is relatively slow, i.e., 250 M^{-1} s^{-1}, following a dissociative mechanism, as proved by its activation volume of +17.4 cm^3 mol^{-1}, close to the theoretical limit of complete loss of a water molecule, i.e., partial molar volume of a bulk solvent (water) molecule [31]. In table 1, it is also

Table 1. Equilibrium and second-order rate constants for some nitrosyl complex formation reactions.

	Complex[a]	k_f (M^{-1} s^{-1})	K_f (M^{-1})	Ref.
1	$Fe(TPEN)^{2+}$	8.4×10^3	5.6×10^2	This work
2	$Fe(TPPN)^{2+}$	9.3×10^3	5.2×10^2	This work
3	$Fe(EDTA)^{2-}$	2.4×10^8	2.1×10^6	[7]
4	$Fe(HEDTRA)^{-}$	6.1×10^7	1.1×10^7	[7]
5	$Fe(NTA)^{-}$	2.1×10^7	1.8×10^6	[7]
6	$Fe(DTPA)^{3-}$	1.1×10^7	3.0×10^6	[34]
7	$Fe_2(TTHA)^{2-}$	3.5×10^6	3.0×10^7	[34]
8	$Fe(TTHA)^{4-}$	1.0×10^6	4.0×10^6	[34]
9	Fe(MIDA)	8.5×10^5	9.5×10^3	[7]
10	$Fe(MIDA)_2^{2+}$	1.8×10^6	2.2×10^4	[7]
11	$Fe(H_2O)_2^{2+}$	1.6×10^6	1.2×10^3	[34]
12	$Fe(CN)_5(H_2O)^{3-}$[b]	2.5×10^2	1.6×10^7	[31]
13	$Fe(bipy)_3^{2+}$[c]	7.7×10^{-3}		[36]
14	Fe(TPPS)[d]	1.5×10^9	*ca.* 1.0×10^{12}	[37]

[a]All Fe(II) complexes, measured at pH 5.0 otherwise noted.
[b]pH 7.0.
[c]Reaction with CN^-.
[d]pH 7.0.

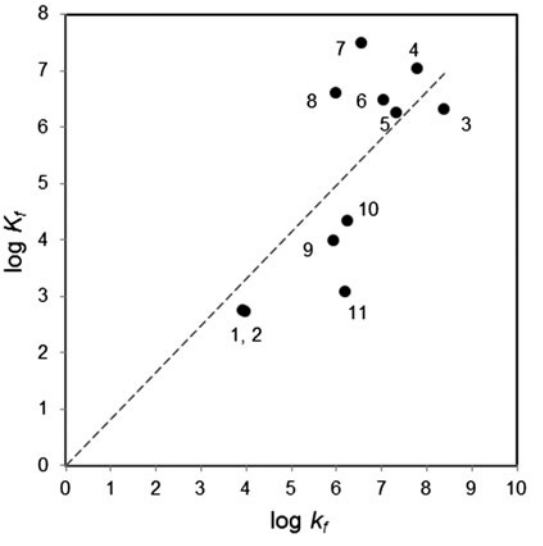

Figure 5. Free energy relationship for the studied complexes $[Fe(TPEN)]^{2+}$ (1) and $[Fe(TPPN)]^{2+}$ (2), and some aminocarboxylate complexes (see table 1 for numbering and references).

possible to observe that the high-spin aminocarboxylate complexes, with $S = 2$ ground state, exhibit a second-order rate constant for the reaction with NO from 2×10^8 to 1×10^6 M^{-1} s^{-1}, several orders of magnitude higher than the other complexes. Figure 5 shows a linear free-energy relationship, i.e., logarithmic plot of equilibrium *versus* rate constants for the nitrosyl complex formations. Although the plot shows appreciable spread due to specific effects within the aminocarboxylate complexes [7, 34], the data corresponding to $[Fe(TPEN)]^{2+}$ and $[Fe(TPPN)]^{2+}$ fall within the correlation, giving evidence that a similar mechanism is operative. The $Fe^{II}(TPPS)$, $[Fe(bipy)_3]^{2+}$, and $[Fe^{II}(CN)_5(H_2O)]^{3-}$ complexes, already discussed, are outliers in this correlation and were not included. As expressed in the Introduction, both $[Fe(TPEN)]^{2+}$ and $[Fe(TPPN)]^{2+}$ are spin-crossover systems with transition temperatures 369 and 385 K, respectively [18, 21]. This means that at 298 K, a small fraction is present in the high-spin state. It is important to note that the $[Fe(TPTN)]^{2+}$ complex, which is low spin up to 400 K [18, 21], did not show any appreciable reaction toward NO.

Following the ideas discussed above, the proposed mechanism for the NO with $[Fe(TPEN)]^{2+}$ and extended for $[Fe(TPPN)]^{2+}$ is depicted in figure 6. The six-coordinate low-spin structure is proposed based on the crystal structures of these complexes [20, 21], which are octahedral with trigonal distortion, and based on $[Fe(bipy)_3]^{2+}$ and $[Fe(TPTN)]^{2+}$, which are both low-spin octahedral complexes [18, 21, 36].

As discussed above, dissociation of pyridine from a six-coordinate low-spin Fe(II) complex has been proved to proceed very slowly [36]; hence, the active species must be in high-spin state. This is strongly supported by our kinetic data and the linear free energy relationship shown in figure 5. From literature data, both $[Fe(TPEN)]^{2+}$ and $[Fe(TPPN)]^{2+}$ interconvert between high and low spin in the ps time-scale (k_1 and k_{-1}) [17–21] in solution. $[Fe(TPEN)]^{2+}$ is in the low-spin state in solid (crystalline) state [18, 21] up to 400 K. In solution, the high-spin species are probably seven-coordinate, due to greater Fe–N bond

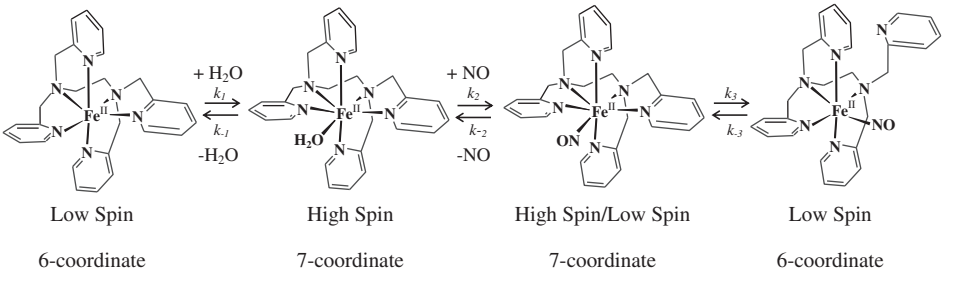

Figure 6. Proposed mechanism for the reaction of $[Fe(TPEN)]^{2+}$ and $[Fe(TPPN)]^{2+}$ with NO.

lengths and trigonal distortions. An analogous high-spin structure for the $[Fe(EDTA)(H_2O)]^{2-}$ complex, which is seven-coordinate with a water molecule, has been resolved through X-ray crystal analysis [39]. If $[Fe(TPEN)]^{2+}$ and $[Fe(TPPN)]^{2+}$ are able to react with NO and other oxygenated species [25–30], as proposed through their high-spin species, then it is reasonable that a solvent molecule is coordinated in solution.

The overall reaction with NO would occur with the release of a pyridyl group or through coordination expansion from 6 to 7 (see figure 6) [8]. A seven-coordinate structure with low-spin ground state has been proposed by Shepherd *et al.* for $[Fe(TPEN)(NO)]^{2+}$, based on the absence of nitrogen hyperfine splitting of the EPR spectrum, interpreted as the spin localized on Fe instead of on N (Fe^{I}–NO^{+}), and favored by a reduction of the ring strain for all pyridyl donors [8]. Depending on the nature of the ligands and the field strength they exert [8], the nitrosyl complexes may have different ground states [40, 41]. For example, $S = 3/2$ in $[Fe(EDTA)(NO)]^{2-}$ [8]. [Fe(EDAMPDA)NO] (EDAMPDA = *N,N′*-bis(pyridylmethyl)-ethylenediamine-*N,N′*-diacetate) exhibits a spin-crossover mixture between $S = 1/2$ and $S = 3/2$ at 106 K [9]. According to Shepherd *et al.*, $[Fe(TPEN)(NO)]^{2+}$ is in the low-spin $S = 1/2$ state at 105 K [8]. However, the dissociation reaction of these complexes, k_d, were found to be 15.6 and 17.7 s^{-1} for $[Fe(TPEN)(NO)]^{2+}$ and $[Fe(TPPN)(NO)]^{2+}$, respectively, which are very similar to those previously found for aminocarboxylate complexes ranging from 91 to 0.1 s^{-1} [7, 34]. Based on this information and the inertness of the Fe(II) low-spin complexes, we propose that $[Fe(TPEN)(NO)]^{2+}$ and $[Fe(TPPN)(NO)]^{2+}$ should be in equilibrium with their corresponding high-spin states at room temperature, to account for the rate of dissociation. Our EPR spectrum of $[Fe(TPEN)(NO)]^{2+}$ shows appreciable amounts of a high-spin species ($S = 3/2$ state) at 132 K, supporting this hypothesis [13]. Alternatively, we should not discard steric and electronic effects which could account for the labilization of the NO ligand in a seven-coordinate low-spin nitrosyl complex. Finally, a possible low-spin six-coordinate structure ($S = 1/2$) with one uncoordinated pyridyl group should be considered, which could be present in equilibrium at low concentration, induced by protonation at low pH.

From the mechanism displayed in figure 6, assuming k_1, k_{-1}, k_3, and k_{-3} as fast reactions [18–21], defining the overall rate of reaction as the formation of both nitrosylated species and taking the high-spin aquo-complex under stationary state kinetic condition, k_{obs} can be expressed as a function of the rate constants of the elementary steps, equation (4).

$$k_{obs} = K_1 k_2 [NO] + k_{-2} \tag{4}$$

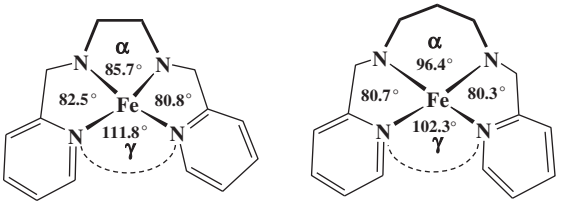

Figure 7. Scheme of the basal planes of $[Fe(TPEN)]^{2+}$ (left) and $[Fe(TPTN)]^{2+}$ (right) obtained from reported crystal structures [20, 42].

In equation (4), $K_1 = k_1/k_{-1}$, $k_f = K_1k_2$, and $k_d = k_{-2}$. The high-spin fraction ([high spin]/[low spin]) was calculated as 0.02 from magnetic susceptibility data for $[Fe(TPEN)]^{2+}$ [17]; this value should equal K_1. This strongly supports the two orders of magnitude lower rate constant observed with the $[Fe(TPEN)]^{2+}$ and $[Fe(TPPN)]^{2+}$ complexes compared with $[Fe(H_2O)_6]^{2+}$. Electronic as well as structural effects influence the rates of reaction and equilibrium constants in aminocarboxylate complexes and prevent a full quantitative analysis [7, 34].

It is important to remark again that $[Fe(TPTN)]^{2+}$ does not react with NO and does not display SOD activity and H_2O_2/O_2 activation either [27]. The rate-determining step of these last-mentioned reactions is coordination of the corresponding oxygenated species, as in the NO reaction [27]. This complex is in the low-spin state and shows a less distorted octahedral geometry [21]. This factor has been proposed to deeply affect the spin interconversion and the rate of racemization [18, 21]. Figure 7 shows the basal or equatorial planes for both $[Fe(TPEN)]^{2+}$ (left) and $[Fe(TPTN)]^{2+}$ (right). It is possible to observe that $[Fe(TPEN)]^{2+}$, which is more distorted from octahedral geometry (with higher spin interconversion rate), has a broader γ angle between the two pyridyl groups, which allows accommodation of a seventh ligand. In contrast, the latter complex, with geometry closer to octahedral (low spin up to 400 K), has reduced space to accommodate a seventh ligand. The angles have been extracted from reported structures [20]. For the TPTN complex, a crystal structure of a Pd complex was employed, since no Fe analog is available [42]. It seems that both electronic and steric considerations influence the reactivity of the complexes under study.

5. Conclusions and future work

The reactions between NO and $[Fe(TPEN)]^{2+}$, $[Fe(TPPN)]^{2+}$, and $[Fe(TPTN)]^{2+}$ were studied by stopped-flow methods. The first two compounds, which are spin-crossover systems, readily react with NO, showing second-order rate constants for the nitrosyl complex formation (k_f) between high-spin Fe(II) aminocarboxylate complexes and low-spin complexes. $Fe(TPTN)]^{2+}$, which is in low-spin state up to 400 K, does not show appreciable reaction with NO. The reactivity can also be rationalized in terms of the crystal structures of these complexes and the angles between Fe–N bonds, which eventually allow for accommodation of a seventh ligand in $[Fe(TPEN)]^{2+}$ and $[Fe(TPPN)]^{2+}$, not the case in the other complex. A mechanism was proposed based on structures experimentally determined or proposed by other authors for the intermediates, which accounts for the observed kinetic data. Features at *g ca.* 4 were observed in the EPR spectrum of $[Fe(TPEN)NO]^{2+}$ at 132 K,

giving evidence for the presence of high-spin ($S = 3/2$) nitrosylated species, and supporting the proposed mechanism. Unfortunately, no activation parameters are available yet. These would help to decide whether there is actually a coordinated solvent molecule that dissociates upon reaction with NO, through a dissociative-interchange mechanism (I_d), as in the $[Fe(EDTA)]^{2-}$ case. Alternatively, in the absence of coordinated water molecule, the reaction would proceed directly through an associative mechanism, expanding the coordination from 6 to 7 in an elementary step. Water exchange experiments, usually performed through NMR, would ultimately probe the presence or absence of a coordinated water molecule.

Disclosure statement

No potential conflict of interest was reported by the authors.

Funding

FR was financially supported for his studies in Germany by the National Research Council of Argentina (CONICET) through a doctoral fellowship.

References

[1] L.J. Ignarro. *Angew. Chem. Int. Ed.*, **38**, 1882 (1999).
[2] S. Moncada, R.M.J. Palmer, E.A. Higgs. *Pharmacol. Rev.*, **43**, 109 (1991).
[3] T.J. Houser, M.E. McCarville, G. Zhuo-Ying. *Fuel*, **67**, 642 (1988).
[4] V. Zang, R. van Eldik. *Inorg. Chem.*, **29**, 4462 (1990).
[5] J.F. Demmink, I.C.F. van Gils, A.A.C.M. Beenackers. *Ind. Eng. Chem. Res.*, **36**, 4914 (1997).
[6] T. Schneppensieper, S. Finkler, A. Czap, R. van Eldik, M. Heus, P. Nieuwenhuizen, C. Wreesmann, W. Abma. *Eur. J. Inorg. Chem.*, **2001**, 491 (2001).
[7] T. Schneppensieper, A. Wanat, G. Stochel, R. van Eldik. *Inorg. Chem.*, **41**, 2565 (2002).
[8] R.E. Shepherd, M.A. Sweetland, D.E. Junker. *J. Inorg. Biochem.*, **65**, 1 (1997).
[9] M.S. Ward, R.E. Shepherd. *Inorg. Chim. Acta*, **286**, 197 (1999).
[10] F.V. Wells, S.W. McCann, H.H. Wickman, S.L. Kessel, D.N. Hendrickson, R.D. Feltham. *Inorg. Chem.*, **21**, 2306 (1982).
[11] T.E. Westre, A. Di Cicco, A. Filipponi, C.R. Natoli, B. Hedman, E.I. Solomon, K.O. Hodgson. *J. Am. Chem. Soc.*, **116**, 6757 (1994).
[12] C.A. Brown, M.A. Pavlosky, T.E. Westre, Y. Zhang, B. Hedman, K.O. Hodgson, E.I. Solomon. *J. Am. Chem. Soc.*, **117**, 715 (1995).
[13] C. Hauser, T. Glaser, E. Bill, T. Weyhermüller, K. Wieghardt. *J. Am. Chem. Soc.*, **122**, 4352 (2000).
[14] A.K. Patra, J.M. Rowland, D.S. Marlin, E. Bill, M.M. Olmstead, P.K. Mascharak. *Inorg. Chem.*, **42**, 6812 (2003).
[15] S. Chakraborty, J. Reed, M. Ross, M.J. Nilges, I.D. Petrik, S. Ghosh, S. Hammes-Schiffer, J.T. Sage, Y. Zhang, C.E. Schulz, Y. Lu. *Angew. Chem. Int. Ed.*, **53**, 2417 (2014).
[16] H. Toftlund, S. Yde-Andersen. *Acta Chem. Scand.*, **A 35**, 575 (1981).
[17] H.-R. Chang, J.K. McCusker, H. Toftlund, S.R. Wilson, A.X. Trautwein, H. Winkler, D.N. Hendrickson. *J. Am. Chem. Soc.*, **112**, 6814 (1990).
[18] J.J. McGarvey, I. Lawthers, K. Heremans, H. Toftlund. *Inorg. Chem.*, **29**, 252 (1990).
[19] J.K. McCusker, K.N. Walda, R.C. Dunn, J.D. Simon, D. Magde, D.N. Hendrickson. *J. Am. Chem. Soc.*, **115**, 298 (1993).
[20] X. Solans, L. Ruiz-Ramirez, R. Moreno-Esparza, M. Labrador, A. Escuer. *J. Solid State Chem.*, **109**, 315 (1994).
[21] J.K. McCusker, A.L. Rheingold, D.N. Hendrickson. *Inorg. Chem.*, **35**, 2100 (1996).
[22] G. Chen, G. Espinosa-Perez, A. Zentella-Dehesa, I. Silaghi-Dumitrescu, F. Lara-Ochoa. *Inorg. Chem.*, **39**, 3440 (2000).
[23] G. Chen, R. Liu, I. Silaghi-Dumitrescu, G. Espinosa-Perez, A. Zentella-Dehesa, F. Lara-Ochoa. *Int. J. Quantum Chem.*, **83**, 60 (2001).

[24] H. Paulsen, L. Duelund, H. Winkler, H. Toftlund, A.X. Trautwein. *Inorg. Chem.*, **40**, 2201 (2001).
[25] T. Nagano, T. Hirano, M. Hirobe. *J. Biol. Chem.*, **264**, 9243 (1989).
[26] T. Hirano, M. Hirobe, K. Kobayashi, A. Odani, O. Yamauchi, M. Ohsawa, Y. Satow, T. Nagano. *Chem. Pharm. Bull.*, **48**, 223 (2000).
[27] M. Tamura, Y. Urano, K. Kikuchi, T. Higuchi, M. Hirobe, T. Nagano. *J. Organomet. Chem.*, **611**, 586 (2000).
[28] M. Martinho, F. Banse, J.F. Bartoli, T.A. Mattioli, P. Battioni, O. Horner, S. Bourcier, J.-J. Girerd. *Inorg. Chem.*, **44**, 9592 (2005).
[29] A. Thibon, J.-F. Bartoli, R. Guillot, J. Sainton, M. Martinho, D. Mansuy, F. Banse. *J. Mol. Catal. A: Chem.*, **287**, 115 (2008).
[30] N. Ségaud, E. Anxolabéhère-Mallart, K. Sénéchal-David, L. Acosta-Rueda, M. Robert, F. Banse. *Chem. Sci.*, **6**, 639 (2015).
[31] F. Roncaroli, J.A. Olabe, R. van Eldik. *Inorg. Chem.*, **42**, 4179 (2003).
[32] S. Stoll, A. Schweiger. *J. Magn. Reson.*, **178**, 42 (2006).
[33] K. Meyer, E. Bill, B. Mienert, T. Weyhermuller, K. Wieghardt. *J. Am. Chem. Soc.*, **121**, 4859 (1999).
[34] T. Schneppensieper, A. Wanat, G. Stochel, S. Goldstein, D. Meyerstein, R. van Eldik. *Eur. J. Inorg. Chem.*, **2001**, 2317 (2001).
[35] J. Heinecke, P.C. Ford. *Coord. Chem. Rev.*, **254**, 235 (2010).
[36] J. Burgess. *J. Chem. Soc., Dalton Trans.*, 1061 (1972).
[37] L.E. Laverman, P.C. Ford. *J. Am. Chem. Soc.*, **123**, 11614 (2001).
[38] M.V. Twigg. *Inorg. Chim. Acta*, **10**, 17 (1974).
[39] T. Mizuta, J. Wang, K. Miyoshi. *Bull. Chem. Soc. Jpn.*, **66**, 2547 (1993).
[40] C. Hauser, T. Glaser, E. Bill, T. Weyhermüller, K. Wieghardt. *J. Am. Chem. Soc.*, **122**, 4352 (2000).
[41] C.A. Brown, M.A. Pavlosky, T.E. Westre, Y. Zhang, B. Hedman, K.O. Hodgson, E.I. Solomon. *J. Am. Chem. Soc.*, **117**, 715 (1995).
[42] M. Sokolov, K. Umakoshi, Y. Sasaki. *Inorg. Chem.*, **41**, 6237 (2002).